Chemical Science

ROYAL SOCIETY OF CHEMISTRY

EDGE ARTICLE

View Article Online
View Journal | View Issue

Cite this: *Chem. Sci.*, 2024, **15**, 20523

All publication charges for this article have been paid for by the Royal Society of Chemistry

Received 28th August 2024
Accepted 21st October 2024

DOI: 10.1039/d4sc05766j

rsc.li/chemical-science

Hydroselenation of olefins: elucidating the β-selenium effect†

Gabriel S. Phun, ‡[b] Hannah S. Slocumb, ‡[b] Kirsten J. Ruud, [b] Shaozhen Nie,[c] Cheyenne Antonio,[d] Filipp Furche, *[b] Vy M. Dong *[b] and Xiao-Hui Yang *[ae]

We report a light-promoted hydroselenation of alkenes with high *anti*-Markovnikov selectivity. Blue light activates an aryl diselenide to generate a seleno radical with subsequent addition into an alkene to form a β-seleno carbon radical. Hydrogen atom transfer (HAT) from the selenol to the carbon radical generates the linear selenide with high selectivity in preference to the branched isomer. These studies reveal a unique β-selenium effect, where a selenide β to a carbon radical imparts high *anti*-selectivity for radical addition through delocalization of the HAT transition state.

Introduction

While an element essential to life, selenium remains less investigated relative to earlier chalcogens (oxygen and sulfur). Proteins containing selenocysteine (selenoproteins) participate in essential antioxidant, redox, and metabolic processes. Selenoprotein thioredoxin reductase 1 catalyzes several antioxidant and redox processes *via* selenocysteine and cysteine residues through the formation and cleavage of a Se–S bond (Fig. 1A).[1] Disulfide bonds between neighboring cysteines are generally conformationally unfavorable, but the use of selenocysteines makes the dichalcogen bond viable due to selenium's longer bond lengths.[2] Selenoproteins act as biomarkers for diseases including cancer and diabetes.[3] Recently, abnormal plasma levels of micronutrient selenium were found in patients suffering severe cases of COVID-19.[4] Apart from its occurence in nature, selenides also appear in drug targets.[5] Ethaselen is a potent thioredoxin reductase 1 inhibitor which has undergone phase I clinical trials (Fig. 1A).[6] Selenides show promise as both ligands and catalysts; the Zhao lab established a series of aryl selenide organocatalysts (Fig. 1A) for stereoselective difunctionalizations.[7] Selenides serve as useful alkyl radical precursors;[8] they exhibit higher stability in comparison to other radical precursors (*e.g.*, halides)[9] and thus can be carried through multi-step syntheses.[10] Inoue and coworkers employed phenyl selenide (Fig. 1A) to generate an alkyl radical to achieve a three-component couplingin the construction of resiniferatoxin.[10a] However, this selenide required multi-step preparation from a different radical precursor. These compelling applications for Se motivate the development of new methods to prepare organoselenides, with hydroselenation being an especially attractive strategy.

Hydroselenation is an atom economical approach to add a Se–H bond across a C–C π-bond.[11] Several metal-catalyzed hydroselenations have been developed, mainly using activated alkenes (such as heterobicyclic alkenes,[12a] allenes,[12b] *N*-vinyl lactams,[12c] or α,β-unsaturated thioamides[12d]) or alkynes.[12] Ogawa reported a light-promoted hydroselenation of alkynes, proposing an alkenyl radical intermediate.[13] A number of other light-promoted reactions with selenides are known, including difunctionalizations,[14] couplings,[15] and cyclizations.[16] Our lab communicated the Rh-catalyzed enantioselective hydroselenation of styrenes where we were able to access the Markovnikov-addition products with high stereoselectivity (Fig. 1B).[12e] In this follow up article, we aim to develop a complementary radical-mediated hydroselenation to form the *anti*-Markovnikov product. Several strategies to achieve a radical hydrofunctionalization are known. In the metal–hydride hydrogen atom transfer (MHAT) approach, a metal hydride adds to an alkene to generate a carbon radical, which is intercepted with a reactive carbon center or heteroatom.[17,18] An alternative strategy involves the addition of a heteroatom radical to an alkene, then delivery of an H-atom *via* an H-atom donor such as a silane or thiol. One classic example of this is the thiol-ene click reaction, where an alkene undergoes

[a]*Advanced Research Institute of Multidisciplinary Science, School of Chemistry and Chemical Engineering, Key Laboratory of Medical Molecule Science and Pharmaceutical Engineering, Ministry of Industry and Information Technology, Beijing Institute of Technology, Beijing, 100081, P. R. China. E-mail: xhyang@bit.edu.cn*

[b]*Department of Chemistry, University of California, Irvine, California, 92697, USA. E-mail: filipp.furche@uci.edu; dongv@uci.edu*

[c]*Department of Medicinal Chemistry, Glaxo-Smith-Kline, Collegeville, Pennsylvania, 19426, USA*

[d]*Department of Chemistry, University of California, San Francisco, California, 94143, USA*

[e]*State Key Laboratory of Elemento-Organic Chemistry, Nankai University, Tianjin, 300071, P. R. China*

† Electronic supplementary information (ESI) available. See DOI: https://doi.org/10.1039/d4sc05766j

‡ These authors contributed equally to this work.

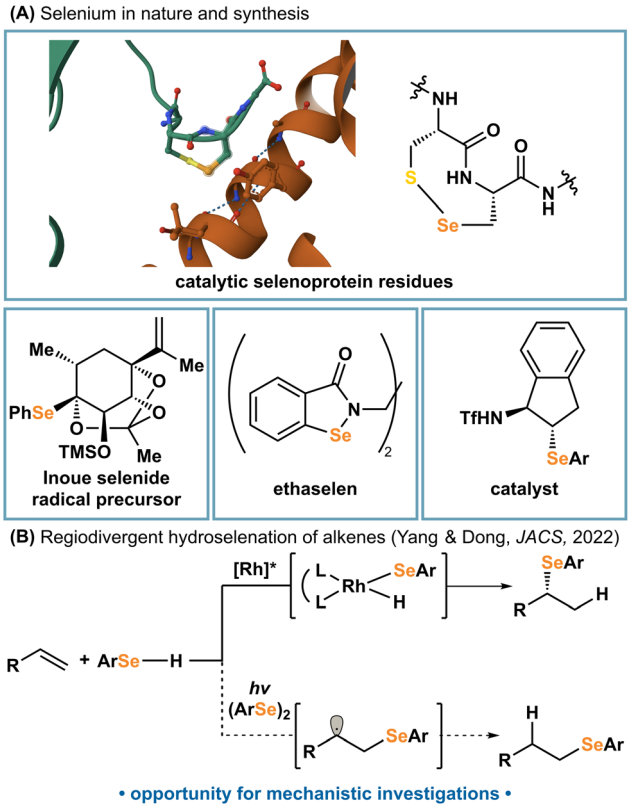

Fig. 1 (A) Selenium in nature (catalytic residues in selenoprotein thioredoxin reductase 1) and synthesis (Inoue seleno radical precursor, ethaselen, and chiral catalyst). (B) Regiodivergent hydroselenation of alkenes *via* Rh (previous work) or light (proposed work).

hydrothiolation with a thiol in the presence of a radical initiator.[19] Within this strategy, the addition of a selenide radical to alkenes has had reports in difunctionalizations featuring the addition of a selenide and C-, N-, O-, S-, F- coupling partners.[14b–d,20] These strategies propose the intermediacy of a β-selenide radical, and either subsequent interception or oxidation. These previous functionalizations often occur with high *anti*-selectivity, yet the origins of this phenomenon remains unexplained. Despite numerous works proposing a β-selenide carbon radical[14,17] and the infamy of the radical thiol-ene reaction, the analogous selenol-ene proceeding through a β-selenide carbon radical has yet to be explored. Herein, we imagined a light-generated seleno radical that would add to the terminal position of an alkene to generate the more stable internal radical, which could then undergo HAT to give the *anti*-Markovnikov selenide (Fig. 1B). If successful, this approach would allow us to (1) access a complementary *anti*-Markovnikov motif, and (2) study the reactivity of the β-seleno radical by both experiment and theory.

Results and discussion

To access the *anti*-Markovnikov product by hydroselenation, we chose feedstock chemical styrene (**1a**) and commercially available benzeneselenol (**2a**) as our model system. The benzeneselenol sample contained 3 mol% diphenyl diselenide (**3a**) due to spontaneous selenol oxidative dimerization.[21] We observed no reactivity when the experiment was performed in the dark (Table 1, entry 1), however under ambient light we found that the hydroselenation can occur to give the *anti*-Markovnikov isomer **4aa** in 15% yield and >20 : 1 rr (Table 1, entry 2). By shining blue LEDs on the reaction mixture and monitoring by TLC, we observed reaction completion and nearly quantitative yield of **4aa** within 20 minutes (Table 1, entry 3). We suspected that the trace diphenyl diselenide **3a** could be the photoactive species promoting reactivity.[13] Indeed, TLC monitoring indicated the reaction time could be shortened to five minutes by adding an additional 20 mol% of diphenyl diselenide (**3a**) (Table 1, entry 4). Together, these results support the critical role of blue light and catalytic diselenide in this coupling.

A condition-based sensitivity screen was performed as outlined by the Glorius group (Fig. 2).[22] Increased oxygen content lowered the yield by 26%. While high intensity of light showed similar results as the optimized conditions, low intensity afforded diminished yield (83%). Slightly lower efficiency is observed at a larger reaction scale (20× optimized conditions, 69% yield).

Synthetic scope

We examined the light-promoted hydroselenation of twenty-eight different alkenes with benzeneselenol (**2a**) to generate the corresponding linear selenides (Fig. 2). Olefin partners were less hazardous and more readily available, so we chose to explore this scope more widely than the selenols. High reactivity and regioselectivity (>20 : 1 rr) are obtained with monosubstituted alkenes (**4ab–4av**, 44–98% yield). Wide functional group tolerance is shown, including halides (**4ab**, **4ad**, **4ae**, **4ah**), acids (**4ak**, **4ao**), and heterocycles (**4ar–4au**). This process can occur with unactivated alkenes (**4av**), in contrast to the activated alkenes required in previous hydroselenations.[12a–e,23] Both 1,1-disubstituted (**4aw–4ay**, 90–94% yield) and 1,2-disubstituted alkenes (**4az–4aab**, 79–93% yield) undergo addition. A conjugated diene undergoes the selenol-ene to afford the homoallylic selenide (**4aac**) with 87% yield and >20 : 1 rr. We

Table 1 Optimization for the *anti*-Markovnikov hydroselenation of styrene using benzeneselenol. Yields are determined by NMR analysis using 1,3,5-trimethoxybenzene as the internal standard

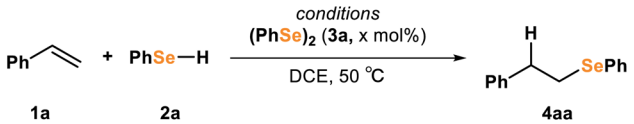

Entry	Conditions	**3a** mol%	Time	Yield
1	Dark	3	24 h	ND
2	Ambient light	3	24 h	15%
3	Blue LEDs	3	20 min	98%
4	Blue LEDs	23	5 min	98%

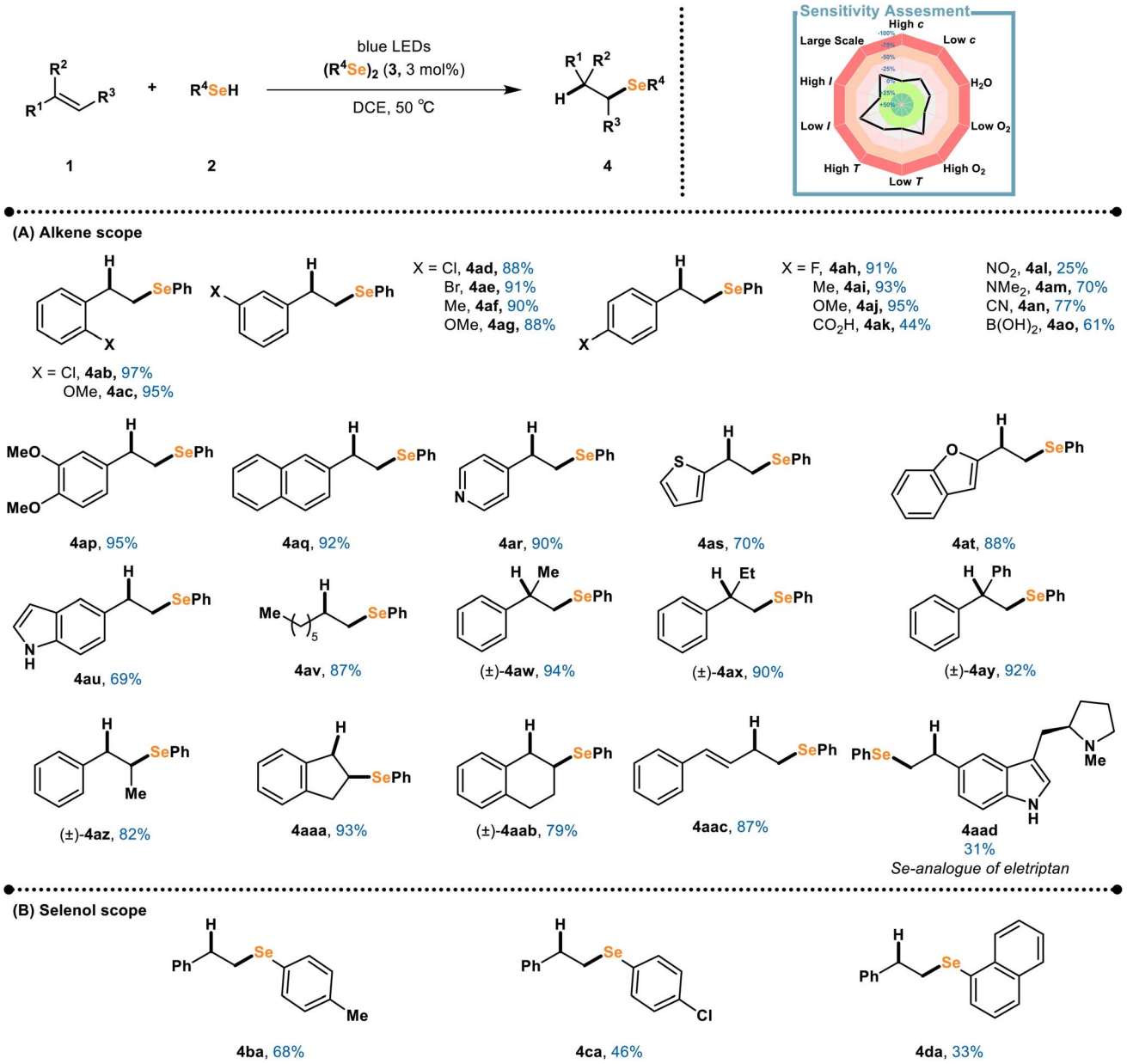

Fig. 2 Scope of light-catalyzed hydroselenation for (A) alkenes and (B) selenols. Reaction conditions for alkene scope: **1** (1.0 equiv.), **2** (1.5 equiv.), 1,2-dichloroethane (0.25 M). Reaction conditions for selenol scope: **1** (1.0 equiv.), **3** (1.5 equiv.), Ph_2POH (1.5 equiv.), 1,2-dichloroethane (0.25 M). Reactions are run in a light box under blue LEDs and monitored by TLC for reaction completion (20 min to 24 h). Temperature in the box rises to 50 °C in 20 minutes due to LEDs and maintains that temperature over time. Regioselectivity determined by ^{1}H NMR analysis of the unpurified reaction mixture.

applied this hydroselenation to prepare a Se-analogue of eletriptan, a migraine medication, which has an $-SO_2Ph$ group instead of the SePh group in **4aad**. The reaction gave a Se-analogue **4aad** in a 31% yield. Several selenols (generated *in situ* from the diselenide and Ph_2POH) provide *anti*-Markovnikov products with high regioselectivity. A more electron-rich aryl selenol (**4ba**, 68% yield) shows higher reactivity compared to an electron-poor aryl selenol (**4ca**, 46% yield). A bulkier, less aromatic selenol had diminished reactivity (**4da**, 33% yield). We hypothesize the lower yielding reactions to form **4ca** and **4da** are due to the heterogeneous character of the solutions, resulting from the precipitation of diphenylphosphinic acid and resulting diphenylphosphinyl selenide byproducts in the dichloroethane (DCE) solvent, which led to low absorption of light. Overall, this light promoted selenol-ene occurs under mild conditions to form linear organoselenides with excellent regiocontrol.

Mechanistic hypotheses

Initially, we investigated the photoactive species of the transformation. UV-visible spectra showed that absorbance in the blue light region corresponds to diphenyl diselenide (Fig. S3†).

Ultra-fast transient absorption spectra also showed identical behavior between diphenyl diselenide (**3a**), the benzeneselenol sample (**2a**), and the reaction mixture (see ESI 5.2 for details†). Based on these spectroscopic results, we concluded that the photoactive species is diselenide (**3**), which is formed by selenols when exposed to light or oxygen.[21] Considering Ogawa's light-promoted hydroselenation of alkynes,[13] we were interested whether this selenol-ene involves radicals. We found that azobisisobutyronitrile (AIBN) could be used as an initiator, giving 54% yield (Fig. 3A). The background reaction at 70 °C gave only 15% yield, highlighting that AIBN effectively promotes hydroselenation. Additionally, a mixture of two distinct diselenides in DCE gave mixed diselenide product when exposed to blue LEDs (Fig. 3B). Thus, AIBN-mediated reactivity and crossover studies indicate the importance of seleno radicals in the reaction. A light–dark study (Fig. S6†) revealed that light is necessary for reaction progress; when the light is off, the reactivity halts, but resumes when re-exposed to light. This observation is consistent with a previous report of high rates of recombination for seleno radicals.[20f]

Diselenide excitation is supported computationally (see ESI 6.2).† Excitation energies of **1a**, **2a**, **3a** and an optimized S_1 state geometry of **3a** were computed using time-dependent density functional theory (TDDFT) to support the feasibility of photoabsorption and photoinduced homolytic cleavage. The excitation energies are consistent with the experimental UV-visible spectra, with **3a** being the only species with a S_1 excitation within range of the blue LEDs. The S_1 state of **3a** has Se–Se σ* character. Upon S_1 state geometry optimization, the Se–Se bond lengthens by 0.47 Å. Moreover, the computed Se–Se bond dissociation energy changes from energetically unfavorable (35.7 kcal mol^{-1}) to favorable (−15.3 kcal mol^{-1}) upon S_1 excitation.

Notably, simply using thiophenol with blue LEDs does not promote reactivity. Likely the reagent does not contain any species with absorptions in the blue LED range. However, by spiking the solution with diphenyl diselenide, we were able to obtain the sulfide product in 81% yield, with 4% selenide product as well (see ESI 5.6).† Deuterium labeling studies revealed high *anti*-selectivity for cyclic selenide **4aab** (Fig. 3C). Similarly, hydroselenation of a tri-substituted acyclic alkene gave high selectivity for a single diastereomer for selenide **4aae** (Fig. 3D). Additionally, deuterium labeling studies with thiophenol revealed high *anti*-selectivity for cyclic sulfide **8aab** (Fig. 3E). High diastereoselectivity is relatively uncommon in radical reactions, so we investigated several potential mechanisms to determine which reflected the observed selectivity.

The importance of diphenyl diselenide and light in the reaction suggests activation of the diselenide **3** by light (Fig. 4). Excited state diselenide **3*** can undergo homolytic bond cleavage to form seleno radical **Ia**. Based on literature precedence,[13] we propose that the radical could then add to alkene **1ab** to form C-radical **IIab**. To investigate the origin of *anti*-selectivity from this β-seleno radical, we proposed three diverging mechanisms: **M1**, a diastereoselective HAT; **M2**, a seleniranium process; and **M3**, a radical selenirane process. Two other mechanisms, involving a Dexter Energy Transfer (DET) event or formation of a styrene radical cation were also

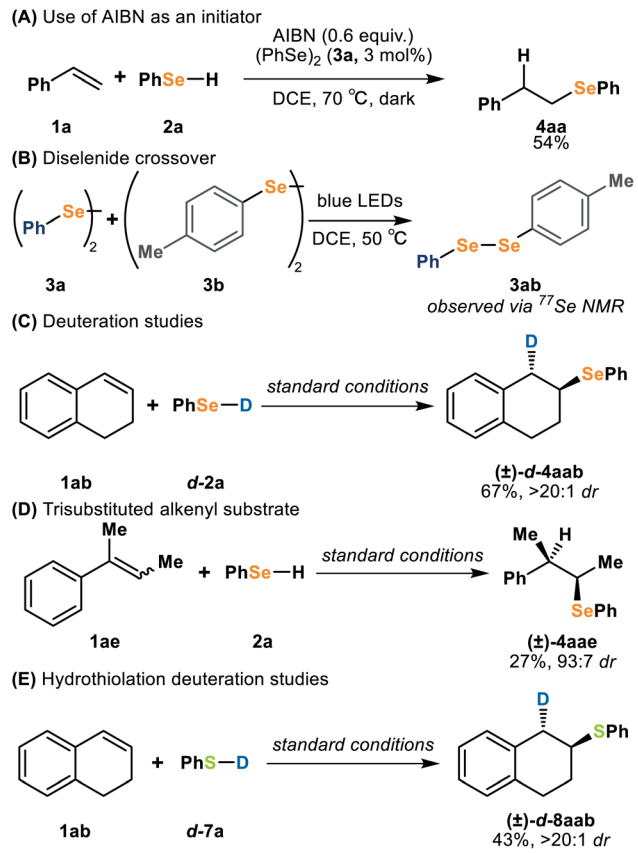

Fig. 3 (A) Reaction run in the dark using AIBN as an initiator; (B) diselenide crossover experiment; (C) *anti*-selective addition of a deuterated selenol to a cyclic styrene; (D) *anti*-selective addition of selenol to a trisubstituted styrene; (E) *anti*-selective addition of a dueterated thiol to a cyclic styrene.

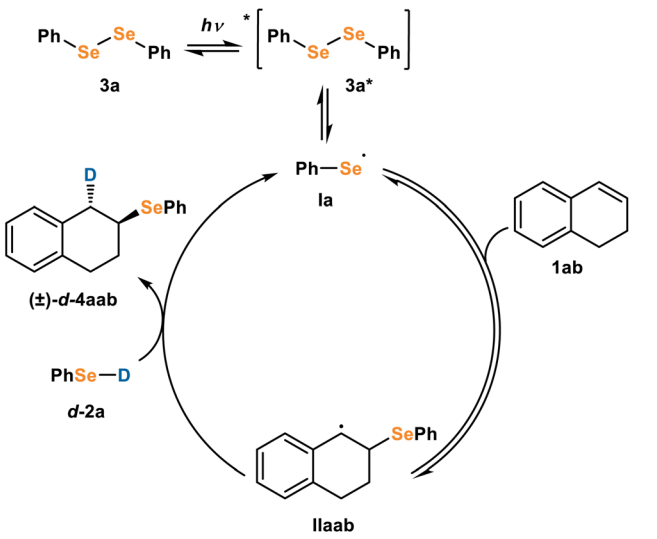

Fig. 4 Favored mechanism for diastereoselective formation of *d*-4aab.

investigated, but these mechanisms favored *syn*-addition and were therefore ruled out (see ESI for details).† We found that **M1** (Fig. 4) is the most likely mechanism, and we herein detail our experimental and computational results which support or refute **M1**, **M2**, and **M3**.

Selective HAT mechanism (M1)

For **M1** (Fig. 4), seleno radical **Ia** adds to the alkene **1ab** to form alkyl radical **IIaab**. We propose a subsequent HAT with selenol *d*-**2a** provides product **4aab**. Concerted addition of radical **Ia** and HAT with selenol *d*-**2a** to alkene **1ab** would be a termolecular reaction which is kinetically unlikely. Ogawa has proposed a similar mechanism where the homolytic bond cleavage of diselenides generates seleno radicals, which undergo addition to alkynes.[13] This mechanism is in accordance with the experimental observation of seleno radicals, but to probe whether the predicted diastereoselectivity reflected the experimental results we turned to computational studies.

Computational studies of M1

We focused our computational studies on analyzing the predicted selectivity for cyclic styrene substrate **1ab**. For **M1**, the diastereo-determining step will be the HAT step; hence we focused on the calculations for the intermediate (**IIaab**), transition state (**TS2**) and product (**4aab**) for that step.

Relative free energies of transition states and intermediates were computed with DFT to predict the diastereomeric ratios (dr) (Fig. 5). It is likely that there is interconversion between the *anti*- and *syn*-isomers of **IIaab**, due to the low barrier of inversion for tetrahedral C-radicals. This profile is the condition for Curtin–Hammett control which results in a dr that only depends on the transition state free energies rather than the activation energies. The computed *anti*- to *syn*-product ratio is >99 : 1 dr, which corresponds well with the experimentally observed >20 : 1 dr. In the less likely scenario where there is not facile interconversion of *anti*- and *syn*-**IIaab**, the reaction would be under kinetic control and therefore depend upon the $\Delta\Delta G$ between *anti*- and *syn*-**IIaab**. In this case, calculations also indicate a >99 : 1 dr, and still support experimental results.

Comparing the singly occupied molecular orbitals (SOMOs) of the HAT step transition state (**TS2**) reveals a qualitative difference between the *syn*- and *anti*-**TS2** electron densities (Fig. 6). The SOMO of the *anti*-**TS2** is delocalized a greater distance because selenium atoms are more linear. The SOMO of both transition state structures has weak C–H bonding and Se–H antibonding character (Fig. 6). However, the almost linear (133°) Se–C–C configuration over 5.5 Å in the *anti*-**TS2** structure affords additional stabilization of the SOMO by hyperconjugation with the σ* orbital of the adjacent C–Se bond, whereas the 77° Se–C–C angle reduces the length scale of delocalization (3.74 Å) in the *syn*-**TS2** structure. The *anti*-**TS2** SOMO delocalization shows some antibonding character and results in a small lengthening in the *anti*-**TS2** β-Se–C bond (2.005 Å) compared to the *syn*-**TS2** β-Se–C bond (2.003 Å). Based on these results, it is likely that electronic effects contribute greatly to give the high *anti*-selectivity. Sterics may also have an impact,[20l] however steric effects alone would not explain the observed bond lengthening and extended delocalization.

We were interested in the high diastereoselectivity observed for acyclic product **4aae**. DFT calculations were performed on the entire reaction coordinate (see ESI).† Calculations indicated a high *anti*-selectivity in this case as well. However, both (*E*)- and (*Z*)-**1ae** give the same diastereomer experimentally, which was found to be the product of *anti*-addition to (*E*)-**1ae**. Depletion of (*E*)-**1ae** occurs more quickly in the reaction, and isomerization between the two alkenes under reaction conditions is also observed. Thus, it is possible that there is a pre-equilibrium between the alkenes followed by a faster *anti*-addition reaction to (*E*)-**1ae**. The calculations do not fully describe a significantly faster reaction with (*E*)-**1ae**, but do support high *anti*-selectivity in a similar fashion to the cyclic system.

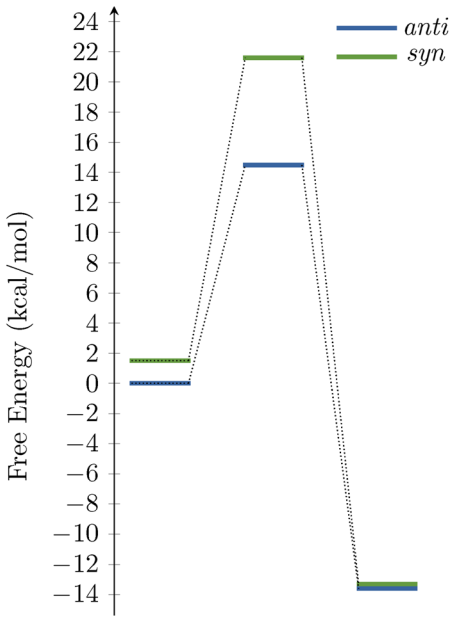

Fig. 5 Energies of the intermediate **IIaab** and HAT transition state (**TS2**) for *syn*- and *anti*-addition. Energies are: *anti*-**IIaab**, 0 kcal mol^{-1}; *syn*-**IIaab**, 1.51 kcal mol^{-1}; *anti*-**TS2**, 14.48 kcal mol^{-1}; *syn*-**TS2**, 23.01 kcal mol^{-1}; *anti*-**4aab**, −13.60 kcal mol^{-1}; *syn*-**4aab**, −13.30 kcal mol^{-1}.

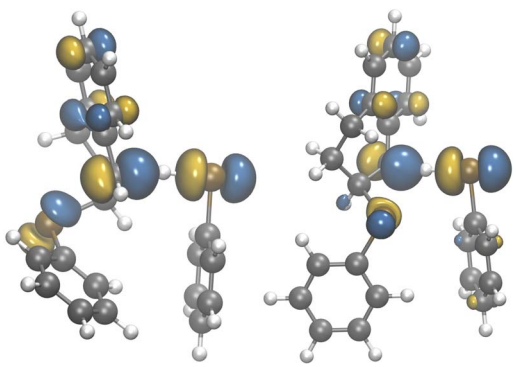

Fig. 6 SOMO of the *anti*- and *syn*-HAT transition states (**TS2**).

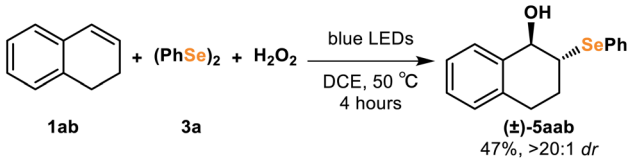

Scheme 1 Use of H_2O_2 as a radical trap reagent.

Based on our observed diastereoselectivity and computational investigations, we propose a novel "β-selenium effect" for radical additions due to delocalization of the transition state SOMO. This effect is an exciting parallel to the β-silicon effect.[24] Further, our present results suggest that the β-selenium effect arises from delocalization rather than a seleniranium intermediate.[25]

We were interested in whether the β-selenium effect extends to other radical additions, so we investigated whether the C-radical can be trapped using H_2O_2. This type of reactivity is analogous to work in hydrodesulfurization.[26] We found that a mixture of alkene **1ab**, **3a**, and H_2O_2 gave sole *anti*-addition (Scheme 1).

From these studies, we conclude that the β-selenium effect is applicable to trapping of C-radicals β to a selenide with high stereocontrol.

Seleniranium mechanism (M2)

Mechanisms involving seleniraniums are well precedented.[27] The addition of an electrophilic selenium moiety to an alkene forms a seleniranium, which can subsequently be opened by a range of nucleophiles. Addition of the nucleophile occurs with *anti*-selectivity. This reactivity includes applications such as polyene cyclizations,[27b] selenoetherifications[28] and selenolactonizations.[29] Strong evidence for seleniraniums has been observed, as the seleniranium ion structure has recently been thoroughly characterized.[30] Based on this literature precedence and the observed *anti*-selectivity, we were curious whether our selenol-ene occurs *via* a seleniranium intermediate. In this proposed mechanism (Fig. 7), C-radical intermediate **IIaab** can be oxidized to form seleniranium intermediate **IIIaab**. Subsequent HAT and reduction (order is unknown so they are drawn as a single step) can give the product **4aab** and regenerate seleno radical **Ia**. To probe this mechanism, we imagined independently synthesizing a seleniranium and subjecting it to the reaction conditions, but the instability of seleniraniums precluded their use at reaction temperature.[28b,30]

To form the seleniranium, oxidation is required and so, we investigated the presence of oxidants in the reaction. There are two possible mechanisms for oxidation: first, C-radical **II** can be oxidized to form a carbocation followed by ring closing to form **III** (Fig. 8A), or ring closing can occur first to form the radical selenirane **IV** followed by oxidation to form **III** (Fig. 8B).

Based upon previous redox studies of benzeneselenol, styrene, and diphenyl diselenide, we realized that the ground state species of these reagents were unable to facilitate oxidation.[31] Therefore, we calculated the redox potentials of various excited-state species in the reaction. The $\mathbf{1e}^-$ reduction potential for seleno radical **Ia** is calculated to be −4.46 eV. For the carbocation pathway (Fig. 8A), the oxidation of the C-radical intermediate **IIaa** is +5.13 eV (Table 2). Based on these calculations, the redox event using a seleno radical **Ia** as an oxidant for **IIaa** is energetically uphill and therefore unlikely (Fig. 8C). DFT studies of the neutral selenirane radical indicated that this was not an energetically feasible intermediate (*vide infra*).

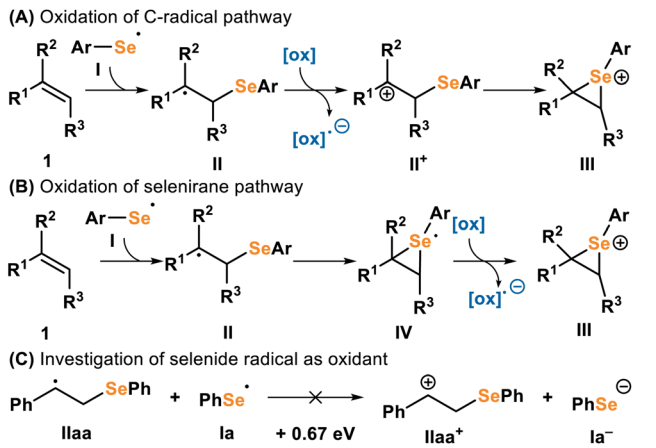

Fig. 8 (A) Oxidation pathway involving carbocation; (B) oxidation pathway involving selenirane; (C) investigated oxidation of C-radical.

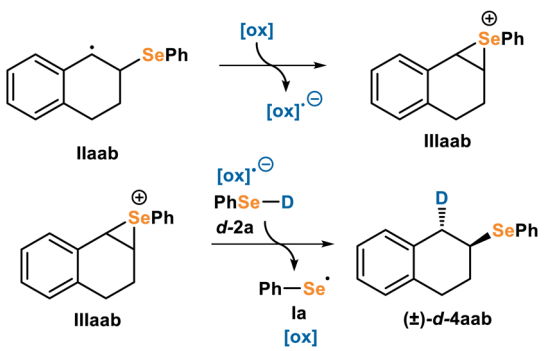

Fig. 7 Proposed seleniranium mechanism (M2) for formation of *anti*-*d*-4aab starting from carbon radical IIaab.

Table 2 Energy differences for redox processes of radical intermediates

	Ia → Ia$^{\bullet-}$	IIaa → IIaa$^+$
Adiabatic electronic energy difference	−4.46 eV	5.13 eV

Table 3 NMR yields of product after three minutes using triphenylmethane as internal standard. Reaction conditions: **1a** (0.1 mmol), **2a** (0.15 mmol), solvent (0.167 M), blue LED irradiation for three minutes

	Inert	Air	O_2 balloon
Yield (μmol)	72.1 ± 4.5	73.2 ± 4.6	74.4 ± 4.6

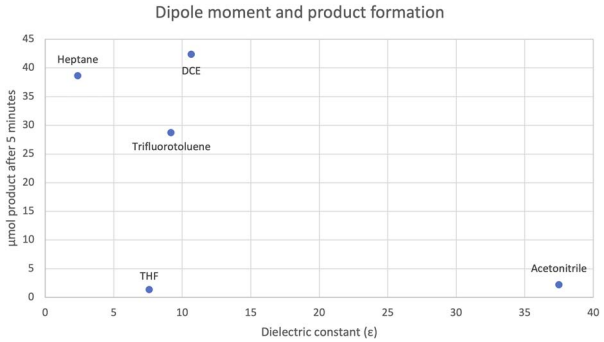

Fig. 9 Observed lack of trend between dielectric constant and product formation early in the reaction. Tested solvents included heptane, 1,2-dichloroethane, α,α,α-trifluorotoluene, tetrahydrofuran, and acetonitrile. Reaction conditions: **1a** (0.1 mmol), **2a** (0.15 mmol), solvent (0.25 M), blue LED irradiation for five minutes. Yield measured using GC-FID analysis with trimethoxybenzene as internal standard.

To investigate whether oxygen could be the oxidant, parallel experiments were run: one under inert conditions (<5.0 ppm O_2), one under brief exposure to the atmosphere, and one under an O_2 balloon. All three reactions proceeded similarly, and the reaction occurred in the absence of O_2; therefore, we concluded that O_2 is unlikely to affect reactivity (Table 3).

Further, we investigated the impact of solvent dielectric constant on reaction rate. Based on Marcus theory,[32] if redox reactivity occurred to form a seleniranium, the reaction should be faster in solvents with higher dielectric constants. A higher solvent dielectric constant allows for rapid solvent reorganization upon charged species formation. However, we observed no correlation between solvent dielectric constant and yield at an early time point in the reaction (Fig. 9). In fact, acetonitrile, which has the highest dielectric constant and smallest radius, led to one of the lowest yields early in the reaction. Therefore, it is unlikely that charged species formation occurs during this reaction.

Based on these mechanistic studies, we were able to conclude that the presence of oxidants and ionized intermediates is unlikely. Therefore, a seleniranium mechanism for this reaction is improbable.

Selenirane mechanism (M3)

After establishing **M2** is unlikely, we imagined a similar mechanism involving a neutral selenirane (Fig. 10).

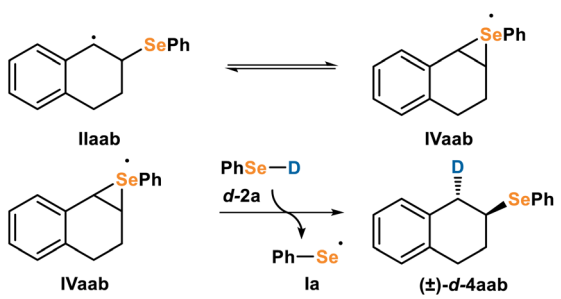

Fig. 10 Proposed radical selenirane mechanism (M3) for formation of *anti-d*-4aab starting from carbon radical IIaab.

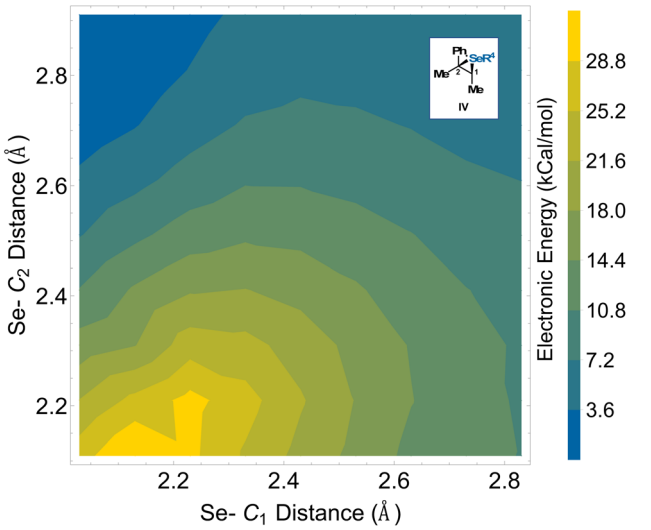

Fig. 11 Potential energy surface scan of selenirane mechanism. No minima (intermediates) or saddle points (transition states) were found corresponding to a selenirane.

In this mechanism, C-centered radical **IIaab** could be in equilibrium with the Se-centered radical selenirane **IVaab**, and could undergo HAT with selenol **2a** to give the product **4aab** and regenerate seleno radical **Ia**. This pathway would similarly have high *anti*-selectivity but would not require redox activity. A similar structure has been proposed by Beckwith in thiol-oxygen cooxidation reactions.[26g] We investigated **M3** computationally to determine the energetic feasibility. A potential energy surface scan of **IV** (Fig. 11) varying the Se–C1 and Se–C2 bond lengths showed no local minimum that corresponded to the selenirane ring and no saddle points that would correspond to a transition state (Fig. 11). The lack of energetically feasible intermediates or transition states for a radical selenirane indicates that **M3** is unlikely to be the operative mechanism.

Conclusions

The generation of carbon radicals from alkenes is an exciting approach to hydrofunctionalization. This strategy can be achieved through (1) metal–hydride hydrogen atom transfer (MHAT);[30] (2) generation of radical cations from alkenes;[31] or (3) the addition of a heteroatom radical to alkenes.[32] We report a novel hydroselenation falling under this third approach, where a selenide radical adds to an alkene. Using blue LEDs, we were able to access novel selenides. The transformation proceeds with a variety of substrates, including unactivated alkenes and drug-like molecules. The exploration of several potential mechanisms (Table 4) led us to identify a mechanism involving a C-radical as the most likely pathway (**M1**).

Through computational studies, we have been able to identify a novel β-selenium effect which leads to high *anti*-selectivity for trapping C-radicals β to a selenide. In previous studies, sterics have been proposed to impact selectivity of addition to β-carbon radicals; however, through computational studies we have been able to elucidate additional electronic factors which

Table 4 Summary of investigated mechanisms and their agreement or disagreement with experimental and computational results

		M1	M2	M3
Experimental evidence	*anti*-Addition	✓	✓	✓
	Radical evidence	✓	✓	✓
	No rate correlation with polarity of solvent	✓	✗	✓
Computational evidence	Energetically feasible	✓	✗	✓
	Found transition states	✓	N/A	✗
	Favors *anti*-addition	✓	✓	✓

play a significant role in selectivity. This relatively strong stereoelectronic effect appears to be caused by the much greater energetic accessibility of C–Se σ* orbitals compared to other C–X σ bonds with second-row elements. We hope that the application of the β-selenium effect can aid in future stereoselective syntheses, and we expect insights from this study will help to guide future work in hydroselenation and functionalization of selenides.

Methods

Computational methods

All calculations were performed using Turbomole.[33] The molecular geometries were optimized using the DFT functional PBE0,[34] the triple ζ quality def2-TZVP basis set,[35] resolution-of-the-identity approximation (RI),[36] D3 dispersion corrections,[37] and COSMO with a dielectric constant of 10.45 corresponding to DCE.[38] GKS-RPA[39] single point calculations using the DFT functional PBE were then done on these optimized geometries and adiabatic electronic energies using the resolution-of-identity random phase approximation (RI-RPA),[40] 60 frequency quadrature points, triple ζ quality def2-TZVP basis set, an SCF convergence threshold of 10^{-8} Hartree, and grids of size 6 for functional integrations. Finally, the free energy corrections were computed using the "Thermo submodule" of *x*TB.[41]

Experimental methods

Alkene scope. In a N_2-filled glovebox, benzeneselenol (**2a**, 0.15 mmol, 1.5 equiv.) containing 3 mol% diphenyl diselenide (**3a**) was added to a solution of alkene (**1**, 0.1 mmol, 1.0 equiv.) in DCE (0.40 mL) in a 1-dram vial. The vial was sealed with a septa cap and brought out from glovebox. During irradiation with blue LEDs, the temperature was allowed to rise due to proximity to the lights, maintaining ∼50 °C after 20 minutes. The reaction mixture was monitored by TLC, and reactions were irradiated until starting material was consumed or the reaction stalled (1–24 h). The resulting mixture was then cooled to room temperature and the solvent was evaporated by rotary evaporation. The regioselectivities were determined by ^{1}H NMR analysis of the unpurified reaction mixture. Isolated yields (obtained by preparative TLC) are reported.

Selenol scope. In a N_2-filled glovebox, diselenide (**3**, 0.15 mmol, 1.5 equiv.) and diphenylphosphine oxide (0.15 mmol, 1.5 equiv.) were weighed in a 1-dram vial. A mixture of diselenide and diphenylphosphine oxide forms selenol *in situ*.[12e] DCE (0.40 mL) and styrene (**1a**, 0.1 mmol, 1.0 equiv.) were added. The vial was sealed with a septa cap and brought out from glovebox. During irradiation with blue LEDs, the temperature was allowed to rise due to proximity to the lights, maintaining ∼50 °C after 20 minutes. The reaction mixture was monitored by TLC, and reactions were irradiated until starting material was consumed or the reaction stalled (1–24 h). The resulting mixture was then cooled to room temperature and the solvent was evaporated by rotary evaporation. The regioselectivities were determined by ^{1}H NMR analysis of the unpurified reaction mixture. Isolated yields (obtained by preparative TLC) are reported.

Author contributions

G. S. P.: investigation, writing – original draft. H. S. S.: investigation, writing – original draft. K. J. R.: investigation, writing – review, editing, and reviewer response. S. N.: conceptualization, investigation. C. A.: investigation. F. F.: funding acquisition, supervision, writing – original draft. V. M. D.: funding acquisition, supervision, writing – original draft. X.-H. Y.: conceptualization, investigation, supervision, writing – original draft.

Data availability

Details regarding experimental procedures and spectral data for all new compounds (PDF) are available in the ESI.†

Conflicts of interest

Principal Investigator Filipp Furche has an equity interest in TURBOMOLE GmbH. The terms of this arrangement have been reviewed and approved by the University of California, Irvine, in accordance with its conflict of interest policies.

Acknowledgements

We thank Dr Dmitry Fishman for his work on the transient absorption spectroscopy. We also thank the UCI mass spectroscopy facility for their work on the high resolution mass spectroscopy data. We thank the Analysis and Testing Center of Beijing Institute of Technology. X.-H. Y. thanks the National Natural Science Foundation of China (No. 22371016 and 22201018), Beijing Natural Science Foundation (No. 2222024), and the National R&D Program of China (No. 2021YFA1401200) for funding. V. M. D. thanks the U.S. National Science Foundation (No. CHE-2247923) and National Institutes of Health

(2R35GM127071) for funding. H. S. S. thanks the National Science Foundation Graduate Research Fellowship (No. DGE-1839285). F. F. thanks the U.S. Department of Energy, Office of Basic Energy Sciences (DE-SC0025405).

Notes and references

1 (*a*) Q. Cheng, T. Sandalova, Y. Lindqvist and E. S. J. Arnér, *J. Biol. Chem.*, 2009, **284**, 3998–4008; (*b*) Q. Cheng, T. Sandalova, Y. Lindqvist and E. S. J. Arnér, *Crystal structure of recombinant rat selenoprotein thioredoxin reductase 1 with oxidized C-terminal tail*, The Research Collaboratory for Structural Bioinformatics Protein Data Bank, 2008, accessed March 2024, **https://www.rcsb.org/structure/3EAO**.

2 S. Gromer, L. Johansson, H. Bauer, L. D. Arscott, S. Rauch, D. P. Ballou, C. H. Williams, R. H. Schirmer and E. S. J. Arnér, *Proc. Natl. Acad. Sci. U. S. A.*, 2003, **100**, 12618–12623.

3 M. Roman, P. Jitaru and C. Barbante, *Metallomics*, 2013, **6**, 25–54.

4 (*a*) A. Moghaddam, R. A. Heller, Q. Sun, J. Seelig, A. Cherkezov, L. Seibert, J. Hackler, P. Seemann, J. Diegmann, M. Pilz, M. Bachmann, W. B. Minich and L. Schomburg, *Nutrients*, 2020, **12**, 2098; (*b*) A. Alkattan, K. Alabdulkareem, A. Kamel, H. Abdelseed, Y. Almutairi and E. Alsalameen, *Alexandria J. Med.*, 2021, **57**, 21–27.

5 For select reviews, see: (*a*) H. Chuai, S. Q. Zhang, H. Bai, J. Li, Y. Wang, J. Sun, E. Wen, J. Zhang and M. Xin, *Eur. J. Med. Chem.*, 2021, **223**, 113621; (*b*) D. Radomska, R. Czarnomysy, D. Radomski and K. Bielawski, *Int. J. Mol. Sci.*, 2021, **22**, 1009; (*c*) W. Ali, R. Benedetti, J. Handzlik, C. Zwergel and C. Battistelli, *Drug Discovery Today*, 2021, **26**, 256–263; (*d*) V. Gandin, P. Khalkar, J. Braude and A. P. Fernandes, *Free Radical Biol. Med.*, 2018, **127**, 80–97; (*e*) A. P. Fernandes and V. Gandin, *Biochim. Biophys. Acta*, 2015, **1850**, 1642–1660.

6 (*a*) L. Wang, Z. Yang, J. Fu, H. Yin, K. Xiong, Q. Tan, H. Jin, J. Li, T. Wang, W. Tang, J. Yin, G. Cai, M. Liu, S. Kehr, K. Becker and H. Zeng, *Free Radical Biol. Med.*, 2012, **52**, 898–908; (*b*) X. Zheng, Y. Chen, M. Bai, Y. Liu, B. Xu, R. Sun and H. Zeng, *Free Radical Biol. Med.*, 2019, **131**, 7–17.

7 For a review, see: (*a*) L. Liao and X. Zhao, *Acc. Chem. Res.*, 2022, **55**, 2439–2453; for select examples, see: (*b*) X. Liu, Y. Liang, J. Ji, J. Luo and X. Zhao, *J. Am. Chem. Soc.*, 2018, **140**, 4782–4786; (*c*) Y. Liang and X. Zhao, *ACS Catal.*, 2019, **9**, 6896–6902; (*d*) Y. Zhang, Y. Liang and X. Zhao, *ACS Catal.*, 2021, **11**, 3755–3761.

8 (*a*) G. Pandey, K. S. Sesha, P. Rao and B. B. V Soma Sekhar, *J. Chem. Soc., Chem. Commun.*, 1993, **21**, 1636–1638; (*b*) G. Pandey, K. S. Sesha Poleswara Rao and K. V. Nageshwar Rao, *J. Org. Chem.*, 1996, **61**, 6799–6804; (*c*) P. Renaud, *Organoselenium Chemistry*, Radical Reactions Using Selenium Precursors, Springer, Berlin, 2000, pp. 81–112.

9 W. R. Bowman, *Organoselenium Chemistry: Synthesis and Reactions*, 2011, pp. 111–146.

10 (*a*) S. Hashimoto, S. I. Katoh, T. Kato, D. Urabe and M. Inoue, *J. Am. Chem. Soc.*, 2017, **139**, 16420–16429; (*b*) D. L. J. Clive, Y. Tao, A. Khodabocus, Y.-J. Wu, A. Gae'tan Angoh, S. M. Bennett, C. N. Boddy, L. Bordeleau, D. Kellner, G. Kleiner, D. S. Middleton, C. J. Nichols, S. R. Richardson and P. G. Vernon, *J. Am. Chem. Soc.*, 1994, **116**, 11275–11286; (*c*) A. Hirose, A. Watanabe, K. Ogino, M. Nagatomo and M. Inoue, *J. Am. Chem. Soc.*, 2021, **143**, 12387–12396; (*d*) P. Yuan and T. Gaich, *Org. Lett.*, 2022, **24**, 4717–4721; (*e*) T. Asaba, Y. Katoh, D. Urabe and M. Inoue, *Angew. Chem., Int. Ed.*, 2015, **54**, 14457–14461; (*f*) W. Zi, W. Xie and D. Ma, *J. Am. Chem. Soc.*, 2012, **134**, 9126–9129.

11 B. M. Trost, *Science*, 1991, **254**, 1471–1477.

12 (*a*) S. Li, Q. Yang, Z. Bian and J. Wang, *Org. Lett.*, 2020, **22**, 2781–2785; (*b*) A. Ogawa, A. Kudo and T. Hirao, *Tetrahedron Lett.*, 1998, **39**, 5213–5216; (*c*) T. Tamai, M. Yoshikawa, S. Higashimae, A. Nomoto and A. Ogawa, *J. Org. Chem.*, 2016, **81**, 324–329; (*d*) H. Tian, H. M. Zhang and L. Yin, *Angew. Chem., Int. Ed.*, 2023, **62**, e202301422; (*e*) H. S. Slocumb, S. Nie, V. M. Dong and X. H. Yang, *J. Am. Chem. Soc.*, 2022, **144**, 18246–18250; (*f*) S. I. Kawaguchi, M. Kotani, S. Atobe, A. Nomoto, M. Sonoda and A. Ogawa, *Organometallics*, 2011, **30**, 6766–6769; (*g*) V. P. Ananikov, D. A. Malyshev, I. P. Beletskaya, G. G. Aleksandrov and I. L. Eremenko, *J. Organomet. Chem.*, 2003, **679**, 162–172; for select reviews: ; (*h*) A. Ishii and N. Nakata, The Mechanism for Transition-Metal-Catalyzed Hydrochalcogenation of Unsaturated Organic Molecules, in *Hydrofunctionalization*, Springer, Berlin, 2011, pp. 21–50; (*i*) A. Ogawa, Transition-Metal-Catalyzed S–H and Se–H Bonds Addition to Unsaturated Molecules, *Hydrofunctionalization*, Springer, Berlin, 2011, pp. 325–360.

13 Y. Kobiki, S. I. Kawaguchi and A. Ogawa, *Tetrahedron Lett.*, 2013, **54**, 5453–5456.

14 (*a*) A. Ogawa, H. Yokoyama, K. Yokoyama, T. Masawaki, N. Kambe and N. Sonoda, *J. Org. Chem.*, 1991, **56**, 5721–5723; (*b*) D. V. Patil, Y. T. Hong, H. Y. Kim and K. Oh, *Org. Lett.*, 2022, **24**, 8465–8469; (*c*) J. Chen, R. Chen, L. Mei, S. Yan, Y. Wu, Q. Li and B. Yuan, *Asian J. Org. Chem.*, 2020, **9**, 181–184; (*d*) G. Q. Liu, C. F. Zhou, Y. Q. Zhang, W. Yi, P. F. Wang, J. Liu and Y. Ling, *Green Chem.*, 2021, **23**, 9968–9973.

15 (*a*) Z. P. Ye, P. J. Xia, F. Liu, Y. Z. Hu, D. Song, J. A. Xiao, P. Huang, H. Y. Xiang, X. Q. Chen and H. Yang, *J. Org. Chem.*, 2020, **85**, 5670–5682; (*b*) V. Rathore and S. Kumar, *Green Chem.*, 2019, **21**, 2670–2676; (*c*) Q. B. Zhang, Y. L. Ban, P. F. Yuan, S. J. Peng, J. G. Fang, L. Z. Wu and Q. Liu, *Green Chem.*, 2017, **19**, 5559–5563.

16 (*a*) X. J. Zhou, H. Y. Liu, Z. Y. Mo, X. L. Ma, Y. Y. Chen, H. T. Tang, Y. M. Pan and Y. L. Xu, *Chem.–Asian J.*, 2020, **15**, 1536–1539; (*b*) H. Sahoo, G. S. Grandhi, I. Ramakrishna and M. Baidya, *Org. Biomol. Chem.*, 2019, **17**, 10163–10166; (*c*) X. L. Ma, Q. Wang, X. Y. Feng, Z. Y. Mo, Y. M. Pan, Y. Y. Chen, M. Xin and Y. L. Xu, *Green Chem.*, 2019, **21**, 3547–3551; (*d*) H. Hou, Y. Sun, Y. Pan, H. Yu, Y. Han, Y. Shi, C. Yan and S. Zhu, *J. Org. Chem.*, 2021, **86**, 1273–1280; (*e*) C. C. Tran, S. I. Kawaguchi, F. Sato, A. Nomoto

and A. Ogawa, *J. Org. Chem.*, 2020, **85**, 7258–7266; (*f*) Q. Shi, P. Li, Y. Zhang and L. Wang, *Org. Chem. Front.*, 2017, **4**, 1322–1330; (*g*) P. Tan, L. Lu, S. Wang, J. Wang, J. Chen, Y. Zhang, L. Xie, S. Yang, J. Chen and Z. Zhang, *J. Org. Chem.*, 2023, **88**, 7245–7255.

17 For select reviews, see: (*a*) S. W. M. Crossley, C. Obradors, R. M. Martinez and R. A. Shenvi, *Chem. Rev.*, 2016, **116**, 8912–9000; (*b*) S. L. Shevick, C. V. Wilson, S. Kotesova, D. Kim, P. L. Holland and R. A. Shenvi, *Chem. Sci.*, 2020, **11**, 12401–12422; (*c*) R. A. Shenvi, J. L. M. Matos and S. A. Green, *Organic Reactions*, 2019, **100**, 383–470; (*d*) For the seminal work on MHAT, see: J. C. Lo, J. Gui, Y. Yabe, C. M. Pan and P. S. Baran, *Nature*, 2014, **516**, 343–348.

18 For a review, see: (*a*) K. A. Margrey and D. A. Nicewicz, *Acc. Chem. Res.*, 2016, **49**, 1997–2006; for select examples, see: (*b*) D. J. Wilger, J. M. M. Grandjean, T. R. Lammert and D. A. Nicewicz, *Nat. Chem.*, 2014, **6**, 720–726; (*c*) T. M. Nguyen and D. A. Nicewicz, *J. Am. Chem. Soc.*, 2013, **135**, 9588–9591; (*d*) N. A. Romero and D. A. Nicewicz, *J. Am. Chem. Soc.*, 2014, **136**, 17024–17035.

19 For select reviews, see: (*a*) A. K. Sinha and D. Equbal, *Asian J. Org. Chem.*, 2019, **8**, 32–47; (*b*) C. E. Hoyle, A. B. Lowe and C. N. Bowman, *Chem. Soc. Rev.*, 2010, **39**, 1355–1387; (*c*) T. Posner, *Ber. Dtsch. Chem. Ges.*, 1905, **38**, 646–657; (*d*) A. J. Musacchio, B. C. Lainhart, X. Zhang, S. G. Naguib, T. C. Sherwood and R. R. Knowles, *Science*, 2017, **355**, 727–730; (*e*) E. Y. Xu, J. Werth, C. B. Roos, A. J. Bendelsmith, M. S. Sigman and R. R. Knowles, *J. Am. Chem. Soc.*, 2022, **144**, 18948–18958; (*f*) M. Teders, C. Henkel, L. Anhäuser, F. Strieth-Kalthoff, A. Gómez-Suárez, R. Kleinmans, A. Kahnt, A. Rentmeister, D. Guldi and F. Glorius, *Nat. Chem.*, 2018, **10**, 981–988; (*g*) A. B. Lowe, *Polym. Chem.*, 2010, **1**, 17–36.

20 (*a*) L. Sun, L. Wang, H. Alhumade, H. Yi, H. Cai and A. Lei, *Org. Lett.*, 2021, **23**, 7724–7729; (*b*) L. Sun, Y. Yuan, M. Yao, H. Wang, D. Wang, M. Gao, Y. H. Chen and A. Lei, *Org. Lett.*, 2019, **21**, 1297–1300; (*c*) S. F. Wu, Y. Yu, Y. Yuan, Z. Li and K. Y. Ye, *Eur. J. Org. Chem.*, 2022, **2022**, e202201032; (*d*) G. Q. Liu, W. Yi, P. F. Wang, J. Liu, M. Ma, D. Y. Hao, L. Ming and Y. Ling, *Green Chem.*, 2021, **23**, 1840–1846; (*e*) F. H. Cui, Y. Hua, Y. M. Lin, J. Fei, L. H. Gao, X. Zhao and H. Xia, *J. Am. Chem. Soc.*, 2022, **144**, 2301–2310; (*f*) O. Ito, *J. Am. Chem. Soc.*, 1983, **105**, 850–853; (*g*) B. Huang, Y. Li, C. Yang and W. Xia, *Green Chem.*, 2020, **22**, 2804–2809; (*h*) Y. Yin, C. Li, K. Sun, Y. Liu and X. Wang, *Chin. J. Org. Chem.*, 2022, **42**, 1431–1437; (*i*) C. Xu, Z. He, X. Kang and Q. Zeng, *Green Chem.*, 2021, **23**, 7544–7548; (*j*) H. Chen, L. Chen, Z. He and Q. Zeng, *Green Chem.*, 2021, **23**, 2624–2627; (*k*) K. Sun, X. Wang, Y. Lv, G. Li, H. Jiao, C. Dai, Y. Li, C. Zhang and L. Liu, *Chem. Commun.*, 2016, **52**, 8471–8474; (*l*) B. Giese, *Angew. Chem., Int. Ed.*, 1983, **22**, 753–764.

21 N. Sonoda, A. Ogawa and F. Recupero, in *Encyclopedia of Reagents for Organic Synthesis*, 2005, DOI: **10.1002/047084289X.RB018.PUB2**.

22 L. Pitzer, F. Schäfers and F. Glorius, *Angew. Chem., Int. Ed.*, 2019, **58**, 8572–8576.

23 B. Srinivas, V. P. Kumar, R. Sridhar, V. P. Reddy, Y. V. D. Nageswar and K. R. Rao, *Helv. Chim. Acta*, 2009, **92**, 1080–1084.

24 S. N. Ushakov and A. M. Itenberg, *Zh. Obshch. Khim.*, 1937, **7**, 2495–2498.

25 For select reviews, see: (*a*) D. D. Roberts and M. G. McLaughlin, *Adv. Synth. Catal.*, 2022, **364**, 2307–2332; (*b*) J. B. Lambert, Y. Zhao, R. W. Emblidge, L. A. Salvador, X. Liu, J. H. So and E. C. Chelius, *Acc. Chem. Res.*, 1999, **32**, 183–190.

26 (*a*) J. E. Hong, Y. Jung, D. Min, M. Jang, S. Kim, J. Park and Y. J. Park, *J. Org. Chem.*, 2022, **87**, 7378–7391; (*b*) H. Ruan, L. G. Meng, L. Zhu and L. Wang, *Adv. Synth. Catal.*, 2019, **361**, 3217–3222; (*c*) S. F. Zhou, X. Pan, Z. H. Zhou, A. Shoberu and J. P. Zou, *J. Org. Chem.*, 2015, **80**, 3682–3687; (*d*) A. Das and K. R. J. Thomas, *ACS Omega*, 2023, **8**, 18275–18289; (*e*) J. Shi, X. W. Gao, Q. X. Tong and J. J. Zhong, *J. Org. Chem.*, 2021, **86**, 12922–12931; (*f*) H. Wang, Q. Lu, C. Qian, C. Liu, W. Liu, K. Chen and A. Lei, *Angew. Chem., Int. Ed.*, 2015, **55**, 1094–1097; (*g*) A. L. J. Beckwith and R. D. Wagner, *J. Org. Chem.*, 1981, **46**, 3638–3645; (*h*) M. S. Kang, J. Y. X. Khoo, Z. Jia and T. Loh, *Green Synth. Catal.*, 2022, **3**, 309–316; (*i*) G. Qin, R. Wang, Z. Cheng, Y. Zhang, B. Wang, Y. Xia, W. Jin and C. Liu, *Green Synth. Catal.*, 2024, **5**, 131–135.

27 For select reviews, see: (*a*) L. Lu, D. Huang, Z. Wang, X. Wang and X. Wu, *Adv. Synth. Catal.*, 2023, **365**, 2310–2331; (*b*) B. Maji, *Adv. Synth. Catal.*, 2019, **361**, 3453–3489; (*c*) V. A. Potapov, M. V. Musalov, M. V. Musalova and S. V. Amosova, *Curr. Org. Chem.*, 2015, **20**, 136–145.

28 (*a*) H. Zhang, S. Lin and E. N. Jacobsen, *J. Am. Chem. Soc.*, 2014, **136**, 16485–16488; (*b*) S. E. Denmark, D. Kalyani and W. R. Collins, *J. Am. Chem. Soc.*, 2010, **132**, 15752–15765; (*c*) J. Y. See, H. Yang, Y. Zhao, M. W. Wong, Z. Ke and Y. Y. Yeung, *ACS Catal.*, 2018, **8**, 850–858.

29 (*a*) D. L. J. Clive and G. Chittattu, *J. Chem. Soc. Chem. Commun.*, 1977, 484–485; (*b*) K. C. Nicolaou and Z. Lysenko, *J. Am. Chem. Soc.*, 1977, **99**, 3185–3187; (*c*) K. C. Nicolaou, S. P. Seitz, W. J. Sipio and J. F. Blount, *J. Am. Chem. Soc.*, 1979, **101**, 3884–3893; (*d*) D. L. J. Clive, C. G. Russell, G. Chittattu and A. Singh, *Tetrahedron*, 1980, **36**, 1399–1408; (*e*) S. E. Denmark and M. G. Edwards, *J. Org. Chem.*, 2006, **71**, 7293–7306; (*f*) W. Niu and Y. Y. Yeung, *Org. Lett.*, 2015, **17**, 1660–1663.

30 (*a*) S. E. Denmark, W. R. Collins and M. D. Cullen, *J. Am. Chem. Soc.*, 2009, **131**, 3490–3492; (*b*) H. Poleschner and K. Seppelt, *Chem.–Eur. J.*, 2018, **24**, 17155–17161; (*c*) J. Bock, C. G. Daniliuc, K. Bergander, C. Mück-Lichtenfeld and U. Hennecke, *Org. Biomol. Chem.*, 2019, **17**, 3181–3185.

31 (*a*) X. Luo, X. Tang, J. Ni, B. Wu, C. Li, M. Shao and Z. Wei, *Chem. Sci.*, 2023, **14**, 1679–1686; (*b*) S. Y. Ren, Q. Zhou, H. Y. Zhou, L. W. Wang, O. M. Mulina, S. A. Paveliev, H. T. Tang, A. O. Terent'ev, Y. M. Pan and X. J. Meng, *J. Org. Chem.*, 2023, **88**, 5760–5771.

32 R. A. Marcus, *J. Chem. Phys.*, 1956, **24**, 966–978.

33 Y. J. Franzke, C. Holzer, J. H. Andersen, T. Begušić, F. Bruder, S. Coriani, F. Della Sala, E. Fabiano, D. A. Fedotov, S. Fürst,

S. Gillhuber, R. Grotjahn, M. Kaupp, M. Kehry, M. Krstić, F. Mack, S. Majumdar, B. D. Nguyen, S. M. Parker, F. Pauly, A. Pausch, E. Perlt, G. S. Phun, A. Rajabi, D. Rappoport, B. Samal, T. Schrader, M. Sharma, E. Tapavicza, R. S. Treß, V. Voora, A. Wodyński, J. M. Yu, B. Zerulla, F. Furche, C. Hättig, M. Sierka, D. P. Tew and F. Weigend, *J. Chem. Theory Comput.*, 2023, **19**, 6859–6890.

34 (*a*) C. Adamo, G. E. Scuseria and V. Barone, *J. Chem. Phys.*, 1999, **111**, 2889–2899; (*b*) J. P. Perdew, M. Ernzerhof and K. Burke, *J. Chem. Phys.*, 1996, **105**, 9982–9985.

35 F. Weigend and R. Ahlrichs, *Phys. Chem. Chem. Phys.*, 2005, **7**, 3297–3305.

36 B. I. Dunlap, J. W. D. Connolly and J. R. Sabin, *J. Chem. Phys.*, 1979, **71**, 3396–3402.

37 S. Grimme, J. Antony, S. Ehrlich and H. Krieg, *J. Chem. Phys.*, 2010, **132**, 46.

38 A. Klamt and G. Schüürmann, *J. Chem. Soc., Perkin Trans. 2*, 1993, 799–805.

39 (*a*) G. P. Chen, V. K. Voora, M. M. Agee, G. Balasubramani and F. Furche, *Annu. Rev. Phys. Chem.*, 2017, **68**, 421–466; (*b*) H. Eshuis, J. E. Bates and F. Furche, *Theor. Chem. Acc.*, 2012, **131**, 1–18; (*c*) V. K. Voora, S. G. Balasubramani and F. Furche, *Phys. Rev. A*, 2019, **99**, 012518.

40 H. Eshuis, J. Yarkony and F. Furche, *J. Chem. Phys.*, 2010, **132**, 37.

41 C. Bannwarth, E. Caldeweyher, S. Ehlert, A. Hansen, P. Pracht, J. Seibert, S. Spicher and S. Grimme, *Wiley Interdiscip. Rev.: Comput. Mol. Sci.*, 2021, **11**, e1493.